Hybrid Beamforming for dual-polarized antenna

Dien Hoa Truong, Luc Deneire, Fabien Ferrero

▶ **To cite this version:**

Dien Hoa Truong, Luc Deneire, Fabien Ferrero. Hybrid Beamforming for dual-polarized antenna. WCNC 2019, Apr 2019, Marrakech, France. pp.1-6, 10.1109/WCNC.2019.8885767 . hal-02106966

HAL Id: hal-02106966
https://hal.science/hal-02106966

Submitted on 23 Apr 2019

HAL is a multi-disciplinary open access archive for the deposit and dissemination of scientific research documents, whether they are published or not. The documents may come from teaching and research institutions in France or abroad, or from public or private research centers.

L'archive ouverte pluridisciplinaire **HAL**, est destinée au dépôt et à la diffusion de documents scientifiques de niveau recherche, publiés ou non, émanant des établissements d'enseignement et de recherche français ou étrangers, des laboratoires publics ou privés.

Hybrid Beamforming for dual-polarized antenna

Dien-Hoa Truong, Luc Deneire, Fabien Ferrero
Universite Côte d'Azur, CNRS
Sophia Antipolis, France
truong@i3s.unice.fr, {deneire, fabien.ferrero}@unice.fr

***Abstract*—Recently, dual-polarized antenna has attracted strong attention in Millimeter wave (mmWave) systems. It provides an additional degree-of-freedom in wireless communication, yielding higher throughput. Nowadays, with the development of antenna technology, dual-polarized large scale antenna arrays can be realized inexpensively. However, several challenges must be addressed when using dual-polarized antennas in practical transmission such as mobile phone rotation and non-ideal polarization isolation. We address these challenges in the frame of dual-polarized hybrid beamformers. In this paper, we analyze the performance of dual-polarized beamforming based on two popular techniques: Beam steering and Orthogonal Matching Pursuit. Three categories of dual-polarized beam steering are analyzed : (1)** *same ray* **: the two polarizations are sent on the same ray, (2)** *different ray - same polarization* **: the two polarizations are sent on different pathes, and the receiver uses the same polarization as the emitter, (3)** *different ray - different polarization* **: the receiver uses the orthogonal polarization w.r.t. the emitter. An algorithm to choose the rays and polarizations to use, taking the mobile rotation into account, is also developed. Moreover, we develop a hybrid beamforming algorithm inspired by Orthogonal Matching Pursuit that approaches the fully digital beamforming data-rate and outperforms beam steering. Its developed version - Orthogonal based Matching Pursuit - is also introduced to reduce the computational complexity and overcome the unavailability of the Angle of Arrival.**

***Index Terms*—MIMO communication, hybrid beamforming, beam steering, Orthogonal Matching Pursuit, dual-polarized antenna, large scale antenna array, mobile communication, mobile rotation, polarization leakage**

I. Introduction

MmWave communication is a very promising candidate technology for the fifth-generation (5G) wireless cellular technology [1]. It enables gigabit data-rate transmission [2] by taking advantage of the large bandwidth resource.

High attenuation in mmWave can be overcome by using very large antenna arrays and implementing beamforming. In the microwave channel, beamforming is usually implemented digitally in baseband while each antenna is connected to one RF chain. However, it is unpractical in mmWave with a large number of antennas due to cost issues. Instead of using digital beamforming, hybrid beamforming [3] has recently been more attractive in mmWave. Hybrid beamforming combines both digital and analog beamforming, using phase-shifters and/or switches at the RF layer [4]. Beam steering is one of the simplest forms of hybrid beamforming [5]. There are some techniques which can reach higher data rate than beam steering but require higher computational complexity e.g. Spatially Sparse Precoding via Orthogonal Matching Pursuit [6].

Dual-polarized antennas can also be added to the system to extend the efficiency via polarization diversity or multiplexing and to reduce the size of the antenna array. Beam steering for dual-polarized antenna was developed in [7]. This algorithm takes into account realistic impairments i.e. mobile rotation and polarization leakage due to antenna depolarization and scattering effects.

Firstly, in this paper, we analyze the data rate of beam steering for dual-polarized on three categories:

- 2 polarized beams of each side are steered in the same path (same ray beam steering).
- 2 polarized beams of each side are steered in different pathes. Transmitted and received beams of each path are co-polarized (different ray co-polarized beam steering).
- 2 polarized beams of each side are steered in different pathes. Transmitted and received beams of each path are cross-polarized (different ray cross-polarized beam steering).

Then, we introduce a new search algorithm that finds the optimal path combination from only one category based on the mobile rotation to reduce the computational complexity of beam steering technique.

Secondly, because the data rate obtained from beam steering is very limited in comparison with the the digital beamforming, we develop a new hybrid beamforming for dual-polarized antenna based on Orthogonal Matching Pursuit (OMP) algorithm. This new algorithm exceeds the beam steering data rate and approaches digital beamforming data rate. Its developed version - Orthogonal based Matching Pursuit (OBMP) - is also introduced. This technique has less computational complexity and does not need the information of Angle of Arrival (AoD).

The following notations are used throughout this paper. $\mathbf{A}$ is a matrix; $\mathbf{a}$ is a vector; $\mathbf{A}^T$, $\mathbf{A}^*$ denote transpose and conjugate transpose of $\mathbf{A}$ respectively; $|\mathbf{A}|$ and $\|\mathbf{A}\|_F$ are its determinant and Frobenius norm; $A \otimes B$ is the Kronecker product of $\mathbf{A}$ and

978-1-5386-7646-2/19/$31.00 ©2019 IEEE

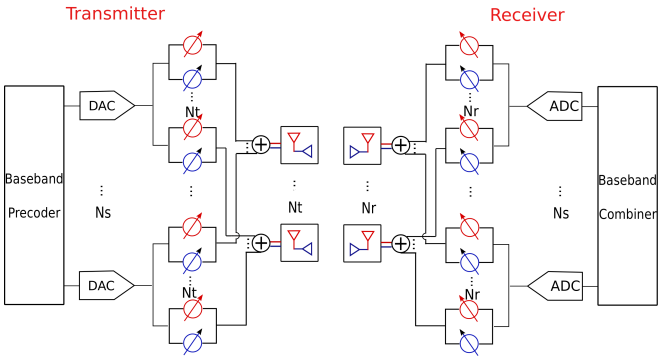

Fig. 1: System Block Diagram

B; expectation is noted by $\mathbb{E}[.]$, $\mathcal{CN}$ is the circularly symmetric complex Gaussian distribution and h,v are respectively horizontal and vertical polarization.

II. System Model

In this section, we present the system model, the dual-polarized mmWave MIMO channel with mobile rotation and polarization leakage.

A. System Model

The dual polarized antenna system is modeled as in [7] consisting of a base station with N_t dual polarized antennas and a mobile station with N_r dual polarized antennas as shown in Fig. 1. For simplicity, we consider a narrowband block-fading channel such that the received signal is :

$$\mathbf{y} = \begin{bmatrix}\mathbf{y}_{\text{h}}^T & \mathbf{y}_{\text{v}}^T\end{bmatrix}^T = \sqrt{\rho}\mathbf{H}\mathbf{F}_{\text{pol}}\mathbf{F}_{\text{BB}}\mathbf{s} + \mathbf{n}, \tag{1}$$

where $\mathbf{s}$ denotes the N_s transmitted symbols with $\mathbb{E}[\mathbf{s}\mathbf{s}^*] = \mathbf{I}_{N_s}/N_s$, $\mathbf{H}$ denotes the $2N_r \times 2N_t$ dual polarized channel matrix satisfying $\mathbb{E}\left[\|\mathbf{H}\|_F^2\right] = 4N_tN_r$. The $2N_t \times N_s$ RF precoder matrix, $\mathbf{F}_{\text{pol}}$, contains both the horizontal precoder $\mathbf{F}_{\text{h}}$ and the vertical precoder $\mathbf{F}_{\text{v}}$ such that $\mathbf{F}_{\text{pol}} = \begin{bmatrix}\mathbf{F}_{\text{h}}^T & \mathbf{F}_{\text{v}}^T\end{bmatrix}^T$. The constraint when using phase-shifters for RF precoder is $\|\mathbf{F}_{\text{pol}}(i,j)\|^2 = \frac{1}{2N_t}$. The baseband precoder $\mathbf{F}_{\text{BB}}$ is a $N_s \times N_s$ matrix that satisfies $\|\mathbf{F}_{BB}\|_F^2 = N_s$, ρ is the average received power and $\mathbf{n}$ is an i.i.d. $\mathcal{CN}(0,\sigma_n^2)$ noise vector. After passing through the RF chains and the phase-shifters at the receiver, we obtain the processed received signal:

$$\tilde{\mathbf{y}} = \sqrt{\rho}\mathbf{W}_{\text{BB}}^*\mathbf{W}_{\text{pol}}^*\mathbf{H}\mathbf{F}_{\text{pol}}\mathbf{F}_{\text{BB}}\mathbf{s} + \mathbf{W}_{\text{BB}}^*\mathbf{W}_{\text{pol}}^*\mathbf{n} \tag{2}$$

Similarly to the precoder, the RF combiner $\mathbf{W}_{\text{pol}} = \begin{bmatrix}\mathbf{W}_{\text{h}}^T & \mathbf{W}_{\text{v}}^T\end{bmatrix}^T$ is a $N_s \times 2N_r$ matrix with constraint $\|\mathbf{W}_{\text{pol}}(i,j)\|^2 = \frac{1}{2N_r}$. $\mathbf{W}_{BB}$ is the baseband combiner matrix with dimension $N_s \times N_s$ and satisfies $\|\mathbf{W}_{BB}\|_F^2 = N_s$. When Gaussian symbols are transmitted over the channel, the spectral efficiency achieved is given by [6] :

$$R = log_2\Big(\Big|\mathbf{I}_{N_s} + \frac{\rho}{N_s}\mathbf{R}_n^{-1}\mathbf{W}_{\text{BB}}^*\mathbf{W}_{\text{pol}}^*\mathbf{H}\mathbf{F}_{\text{pol}}\mathbf{F}_{\text{BB}}\times \mathbf{F}_{\text{BB}}^*\mathbf{F}_{\text{pol}}^*\mathbf{H}^*\mathbf{W}_{\text{pol}}\mathbf{W}_{\text{BB}}\Big|\Big), \tag{3}$$

where $\mathbf{R}_n = \sigma_n^2\mathbf{W}_{\text{BB}}^*\mathbf{W}_{\text{pol}}^*\mathbf{W}_{\text{pol}}\mathbf{W}_{\text{BB}}$ is the noise covariance matrix after combining.

B. Dual-Polarized Channel Model including the effect of mobile rotation

The dual-polarized channel (not including the effect of the rotation of the mobile) $\mathbf{H}_{\text{pol}}$ is composed of 4 blocks $\mathbf{H}_{\text{hh}}$, $\mathbf{H}_{\text{hv}}$, $\mathbf{H}_{\text{vh}}$ and $\mathbf{H}_{\text{vv}}$ corresponding to 4 matching polarizations from receiver to transmitter respectively. The cross-polarization leakage can be modeled by [7] $\varepsilon = \mathbb{E}\left[\|\mathbf{H}_{\text{hv}}\|_F\right]/\mathbb{E}\left[\|\mathbf{H}_{\text{hh}}\|_F\right] = \mathbb{E}\left[\|\mathbf{H}_{\text{vh}}\|_F\right]/\mathbb{E}\left[\|\mathbf{H}_{\text{vv}}\|_F\right]$, hence the polarization isolation is defined as $-10\log_{10}(\epsilon^2)$.

$$\mathbf{H}_{\text{pol}} = \begin{bmatrix}\mathbf{H}_{\text{hh}} & \mathbf{H}_{\text{hv}} \\ \mathbf{H}_{\text{vh}} & \mathbf{H}_{\text{vv}}\end{bmatrix} \tag{4}$$

The clustered channel model based on the extended Saleh Valenzuela is commonly used in mmWave [5]–[7]. In a simple way, each cluster is assumed to contribute a single propagation path. With this model, $\mathbf{H}_{\text{pol}}$ can be expressed as follows :

$$\mathbf{H}_{\text{pol}} = \sqrt{\frac{N_tN_r}{C}}\sum_{i=1}^{C}\begin{bmatrix}\alpha^{hh}(\phi_i^t,\phi_i^r) & \alpha^{hv}(\theta_i^t,\phi_i^r) \\ \alpha^{vh}(\phi_i^t,\theta_i^r) & \alpha^{vv}(\theta_i^t,\theta_i^r)\end{bmatrix} \otimes \mathbf{a_r}(\phi_i^r,\theta_i^r)\mathbf{a_t}(\phi_i^t,\theta_i^t)^*, \tag{5}$$

where C denote the number of clusters, α is the complex gain of the propagation path, $\mathbf{a_r}(\phi_i^r,\theta_i^r)$ and $\mathbf{a_t}(\phi_i^t,\theta_i^t)$ are the receive and transmit array response vectors corresponding to the appropriate angles of arrival and departure. A Uniform Planar Array (UPA) is used in this work as it includes the beamforming in both azimuth and elevation.

The path gain is usually modeled by a circularly symmetric complex Gaussian distribution for omni-directional antennas. In the dual polarized antenna array case, it also depends on the angles (azimuth and elevation) of arrival and departure. It can be written as :

$$\begin{aligned}\alpha^{hh}(\phi_i^t,\phi_i^r) &\sim \mathcal{CN}(0,\sigma^2\cos^2(\phi_i^t)\cos^2(\phi_i^r)) \\ \alpha^{hv}(\theta_i^t,\phi_i^r) &\sim \mathcal{CN}(0,\epsilon^2\sigma^2\cos^2(\theta_i^t)\cos^2(\phi_i^r)) \\ \alpha^{vh}(\phi_i^t,\theta_i^r) &\sim \mathcal{CN}(0,\epsilon^2\sigma^2\cos^2(\phi_i^t)\cos^2(\theta_i^r)) \\ \alpha^{vv}(\theta_i^t,\theta_i^r) &\sim \mathcal{CN}(0,\sigma^2\cos^2(\theta_i^t)\cos^2(\theta_i^r))\end{aligned} \tag{6}$$

The effect of the mobile rotation is modeled by a rotation matrix, composed of 2 rotations. Firstly, the azimuth rotation $\tilde{\phi}$ around z-axis then secondly the elevation rotation $\tilde{\theta}$ around

newly constructed $\tilde{x}$-axis. From [7], we get the equivalent channel model, which includes the mobile rotation as

$$\begin{aligned}\mathbf{H} &= (\mathbf{R} \otimes \mathbf{I}_{N_r})\, \mathbf{H}_{\text{pol}} \\ &= \begin{bmatrix} \cos\tilde{\theta}\cos\tilde{\phi}\mathbf{I}_{\mathbf{N_r}} & \sin\tilde{\theta}\mathbf{I}_{\mathbf{N_r}} \\ -\sin\tilde{\theta}\cos\tilde{\phi}\mathbf{I}_{\mathbf{N_r}} & \cos\tilde{\theta}\mathbf{I}_{\mathbf{N_r}} \end{bmatrix} \begin{bmatrix} \mathbf{H}_{\text{hh}} & \mathbf{H}_{\text{hv}} \\ \mathbf{H}_{\text{vh}} & \mathbf{H}_{\text{vv}} \end{bmatrix}\end{aligned} \tag{7}$$

To ignore the path loss effect, the channel model needs to be normalized by adjusting σ in (6) to guarantee $\mathbb{E}\left[\|\mathbf{H}\|_F^2\right] = 4N_tN_r$.

III. Beam Steering for Dual-Polarized Antenna

A. Conventional beam steering for dual-polarized antenna

From [7], considering the single stream transmission, maximizing the spectral efficiency (3) can be performed by choosing the appropriate polarized beam steering path that maximizes the effective channel gain $\left|\mathbf{W}_{\mathbf{pol}}^{*}\mathbf{H}\mathbf{F}_{\mathbf{pol}}\right|^2$:

$$\begin{aligned}&\Big|\Big(\cos\tilde{\theta}\cos\tilde{\phi}\alpha_{\text{hh}}(p_t^h) + \sin\tilde{\theta}\alpha_{\text{vh}}(p_t^h)\Big)\mathbf{1}(p_t^h = p_r^h) \\ &+ \Big(\cos\tilde{\theta}\cos\tilde{\phi}\alpha_{\text{hv}}(p_t^v) + \sin\tilde{\theta}\alpha_{\text{vv}}(p_t^v)\Big)\mathbf{1}(p_t^v = p_r^h) \\ &+ \Big(-\sin\tilde{\theta}\cos\tilde{\phi}\alpha_{\text{hh}}(p_t^h) + \cos\tilde{\theta}\alpha_{\text{vh}}(p_t^h)\Big)\mathbf{1}(p_t^h = p_r^v) \\ &+ \Big(-\sin\tilde{\theta}\cos\tilde{\phi}\alpha_{\text{hv}}(p_t^v) + \cos\tilde{\theta}\alpha_{\text{vv}}(p_t^v)\Big)\mathbf{1}(p_t^v = p_r^v)\Big|^2,\end{aligned} \tag{8}$$

where p_t^h is the horizontal polarized steering path from the transmitter, similar explanation for p_r^h, p_t^v, p_r^v. $\mathbf{1}(a = b)$ is the indicator function that equals 1 when the condition is satisfied and 0 otherwise.

The total number of path combinations is $(2C-1)C$ and can be classified into 3 categories (Fig. 2) as follows:

- Same path steering: 2 polarized-beams are steered in the same path. The number of path combinations in this case is $\mathbf{C}$.
- Different path, co-polarized steering: we choose the first path from all possible paths and its polarization. Then, we choose the second path from the remaining paths and its polarization which is different from the former polarization. The number of possible combinations is $C(C-1)$.
- Different path, cross-polarized steering: the number of possible combinations is also $C(C-1)$.

In [7], the authors use exhaustive search to find the best combination of path from 3 categories. In the next section, we propose a technique for finding the best combination of paths in just one category based on mobile rotation in order to reduce the computational complexity of the beam steering technique.

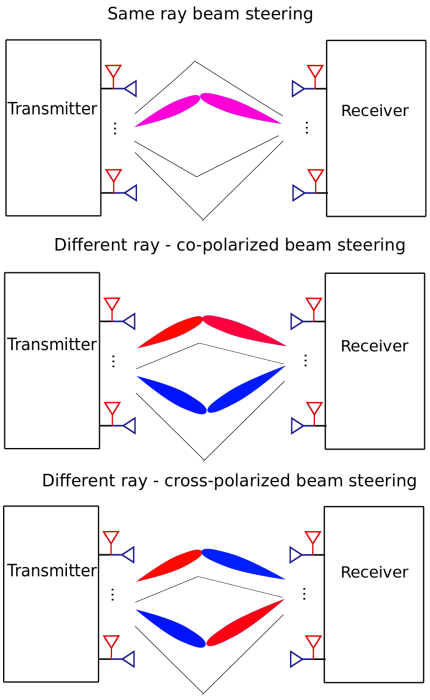

Fig. 2: 3 categories of path combinations in joint polarization beamforming

B. Mobile rotation and choosing the most fitting category

In this section, we analyze the performance of three categories of joint-polarization beamforming based on the mobile rotation.

The mobile rotation can be obtained by using a maximum likelihood estimator (MLE) [7] or the mobile phone's internal sensor. This information can be used to predict the best category to get the highest data-rate in the beam steering dual-polarized beamforming. Hence, the set of path combinations shrinks to only one category.

The effective channel gain of each category depends on the rotation's angle, which is illustrated in Fig. 3. In general, the same ray category has better effective gain than two other categories. However, it has a worse performance in some angles e.g. at $(\pi, \pi/2)$, different ray - cross polarization category has higher data rate than same ray category.

To determine which category should be chosen for path search, boundary of each category is constructed (Fig. 4). Each point illustrates the category which has the highest effective gain depending on mobile rotation. Boundary lines of categories are created by using fitting curve technique with appropriate model function. Boundary 1 and 2 are sinus function, boundary 3 and 4 are 4th order polynomial.

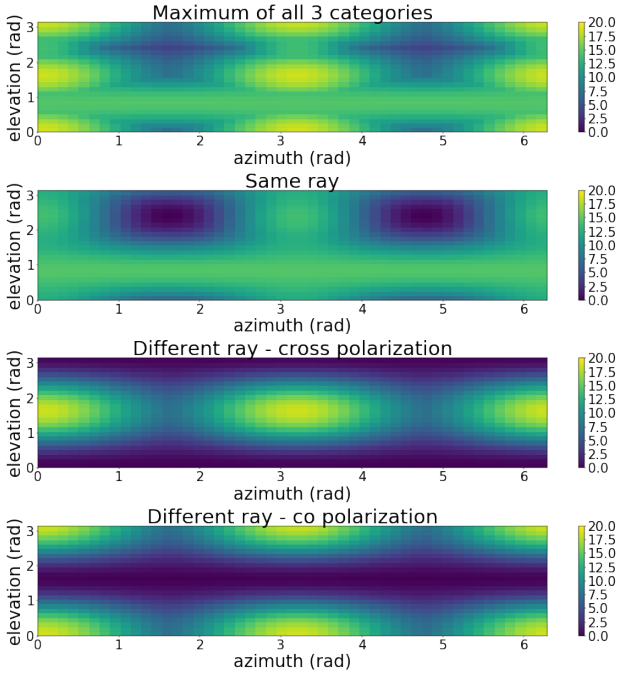

Fig. 3: Effective channel gain of each category depends on mobile rotation

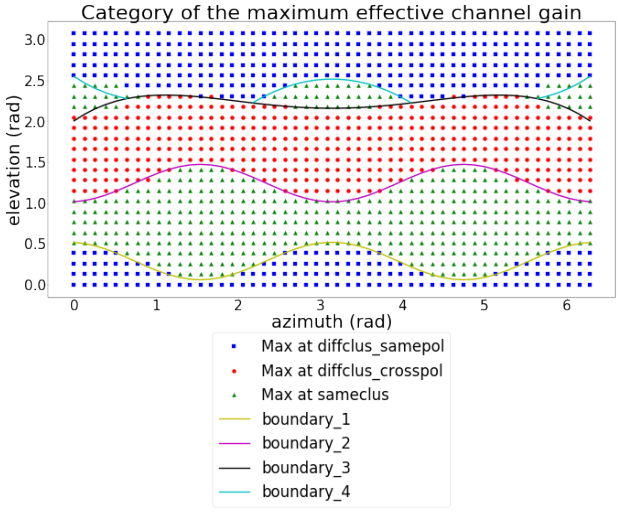

Fig. 4: Category of the maximum effective channel gain depending on mobile rotation and its boundary

IV. Hybrid beamforming based on Orthogonal Matching Pursuit (OMP) for dual-polarized antenna

Beam steering technique works well in the channel with very few number of rays. Its performance reduce when the number of rays increase [8]. In this section, we introduce a new method for beamsteering technique for dual-polarized antenna based on OMP algorithm. Its alternative version to reduce the computational complexity - OBMP - is also proposed.

A. Hybrid beamforming using OMP and OBMP for omnidirectional antenna

Instead of finding $\mathbf{F}_{RF}$ and $\mathbf{F}_{BB}$ that maximizes the spectral efficiency, [8] proposes finding $\mathbf{F}_{RF}\mathbf{F}_{BB}$ close to the optimal precoder (or digital precoder). Then, the optimization problem change from **argmax** R to **argmin** $\|\mathbf{F}_{opt} - \mathbf{F}_{RF}\mathbf{F}_{BB}\|_F$. To reduce further the complexity, the basis vectors of $\mathbf{F}_{RF}$ can be chosen from the array response vectors $a_t(\phi_{il}^t, \phi_{il}^r)$, $\{(\phi_{il}^t, \phi_{il}^r) | 1 \leq i \leq N_{cl}, 1 \leq l \leq N_{ray}\}$ because of its satisfaction for the $\mathbf{F}_{RF}$ constraints.

The problem now is equivalent to a sparse recovery problem which can be solved by a well-known OMP algorithm [9], [10]. The pseudo code is given in Algorithm 1. $\mathbf{A}_t$ is the array response matrix. The algorithm can be summarised as follows. The algorithm starts by projecting the the optimal precoder on the array responses space. Then, the obtained maximum vector $a_t(\phi_{il}^t, \phi_{il}^r)$ will be appended to the RF precoder $\mathbf{F}_{RF}$. In the next steps, the least squares solution of $\mathbf{F}_{BB}$ is calculated and the contribution of the selected vector is removed in order to find other array response vector which has largest projection in the "residual precoding matrix" $\mathbf{F}_{res}$. The process continues until all N_t^{RF} beamforming vector have been selected.

Algorithm 1 Hybrid beamforming using OMP for omnidirectional antenna

Requires: $\mathbf{F}_{opt}$ obtained by SVD

$\mathbf{F}_{RF}$ = Empty Matrix
$\mathbf{F}_{res} = \mathbf{F}_{opt}$
for $i \leq N_t^{RF}$ **do**
  $\mathbf{\Psi} = \mathbf{A}_t^* \mathbf{F}_{res}$
  $k = argmax_{l=1,\ldots,N_{cl}N_{ray}} (\mathbf{\Psi}\mathbf{\Psi}^*)_{l,l}$
  $\mathbf{F}_{RF} = [\mathbf{F}_{RF} \mid A_{t_k}]$
  $\mathbf{F}_{BB} = (\mathbf{F}_{RF}^* \mathbf{F}_{RF})^{-1} \mathbf{F}_{RF}^* \mathbf{F}_{opt}$
  $\mathbf{F}_{res} = \frac{\mathbf{F}_{opt} - \mathbf{F}_{RF}\mathbf{F}_{BB}}{\|\mathbf{F}_{opt} - \mathbf{F}_{RF}\mathbf{F}_{BB}\|_F}$
$\mathbf{F}_{BB} = \sqrt{N_s} \frac{\mathbf{F}_{BB}}{\|\mathbf{F}_{RF}\mathbf{F}_{BB}\|_F}$
return $\mathbf{F}_{RF}$, $\mathbf{F}_{BB}$

In [8], for omnidirectional antenna array system, the data rate of hybrid beamforming using OMP exceeds the data rate of beam steering and approaches the data rate of optimal unconstrained beamforming. However, this algorithm has high computational complexity from the pseudo-inverse process and iterative choosing beamforming basis. The columns in $\mathbf{A}_t$ candidate matrix based on the Angles of Departure (AoD) and they are highly correlated. Therefore, after choosing a column, its correlation must be eliminated before the next iteration. Besides, AoD might

be hard to obtain in the real application. To overcome these limitations, [11] proposes OBMP technique that use orthogonal $N_t \times N_t$ DFT matrix as candidate matrix for $\mathbf{A}_t$ which is called $\mathbf{A}_{DFT}$

$$= \frac{1}{\sqrt{N_t}} \left[1, e^{\frac{-j2\pi(k-1)}{N_t}}, ..., e^{\frac{-j2\pi(k-1)(N_t-2)}{N_t}}, e^{\frac{-j2\pi(k-1)(N_t-1)}{N_t}}\right]^T \tag{9}$$

With this new orthogonal candidate matrix $\mathbf{A}_{DFT}$, finding the best N_t^{RF} steering vectors can be realized parallel and the matrix inversion at each iteration to compute $\mathbf{F}_{BB}$ for $\mathbf{F}_{res}$ can be avoided. The pseudo code of OBMP algorithm is summarized in Algorithm 2.

Algorithm 2 Hybrid beamforming using OBMP for omnidirectional antenna

Requires: $\mathbf{F}_{opt}$ obtained by SVD, candidate matrix A_{DFT}

$\mathbf{\Psi} = \mathbf{A}_{DFT}^* \mathbf{F}_{opt}$
$\mathbf{V}$ = diag($\mathbf{\Psi}\mathbf{\Psi}^*$)
$index = argsort(\mathbf{V})[0 : N_{RF}]$
$\mathbf{F}_{RF} = A_{DFT}[:, index]$
$\mathbf{F}_{BB} = \mathbf{\Psi}[index, :]$
$\mathbf{F}_{BB} = \sqrt{N_s} \frac{\mathbf{F}_{BB}}{\|\mathbf{F}_{RF}\mathbf{F}_{BB}\|_F}$
return $\mathbf{F}_{RF}$, $\mathbf{F}_{BB}$

B. Hybrid beamforming using OMP and OBMP for dual-polarized antenna

To apply OMP algorithm for dual-polarized antenna, the optimization problem is similar to the case with omnidirectionnal antenna - **argmin** $\|\mathbf{F}_{opt} - \mathbf{F}_{RF}\mathbf{F}_{BB}\|_F$. However, the matrix $\mathbf{F}_{opt}$, $\mathbf{F}_{RF}$ and $\mathbf{F}_{BB}$ are now divided into two separable parts: horizontal polarization and vertical polarization. Therefore, two array response vectors for each polarization will be found separately. $\mathbf{F}_{RF}$ is built by stacking these two array response vectors. This technique is summarized by the pseudo code in Algorithm 3.

Based on the idea of separating the precoding matrix into 2 polarization, the algorithm OBMP for dual-polarized antenna is summarized in Algorithm 4. All components in the F_{RF} matrix are found simultaneously and only one pseudo inverse needed.

V. Performance evaluation

In this section, 2 simulations are realized to compare the spectral efficiency of different techniques in 2 scenarios: high number and small number of path rays. The algorithms chosen are optimal beamforming (digital beamforming), exhaustive search beam steering, rotation based search beam steering, hybrid beamforming using, hybrid beamforming using OBMP. A Monte Carlo method is used in this simulation with 1000 channel realizations. 2 cases of channel with 6 clusters, 2 ray per cluster and 6 cluster, 10 rays per cluster. Cluster angle and rotation of the mobile in azimuth and elevation (ϕ,$\tilde{\phi}$ and θ,$\tilde{\theta}$) follow uniform distributions $\mathcal{U}(0, 2\pi)$ and $\mathcal{U}(0, \pi)$ respectively. The polarization isolation is 20dB, corresponding to $\epsilon = 0.1$ which is a common minimum value in antenna design [12]. The UPA antenna system is considered with 8x8 dual-polarized antennas at the transmitter and 4x4 dual-polarized antennas at the receiver. Number of RF chains is $N_{RF} = 6$ and the number of streams is $N_s = 1$. The antenna spacing is half of the signal wavelength ($d = \lambda/2$).

The results are shown in Fig 5 and Fig 6. We find that in the channel with small number of path rays (12 rays), all the represented hybrid beamforming techniques are closed to each other and have big gaps in comparison with the optimal beamforming. In the channel with higher number of path rays (60 rays), OMP technique approaches the optimal beamforming,

Algorithm 3 Hybrid beamforming using OMP for dual-polarized antenna system

Requires: $\mathbf{F}_{opt} = [\mathbf{F}_{h_opt}^T \ \mathbf{F}_{v_opt}^T]^T$ obtained by SVD

$\mathbf{F}_{RF}$ = Empty Matrix
$\mathbf{F}_{res} = [\mathbf{F}_{h_res}^T \ \mathbf{F}_{v_res}^T]^T = \mathbf{F}_{opt}$
for $i \leq N_t^{RF}$ **do**
  $\mathbf{\Psi}_h = \mathbf{A}_t^* \mathbf{F}_{h_res}$
  $k_h = argmax_{l=1,...,N_{cl}N_{ray}} (\mathbf{\Psi}_h \mathbf{\Psi}_h^*)_{l,l}$
  $\mathbf{\Psi}_v = \mathbf{A}_t^* \mathbf{F}_{v_res}$
  $k_v = argmax_{l=1,...,N_{cl}N_{ray}} (\mathbf{\Psi}_v \mathbf{\Psi}_v^*)_{l,l}$
  $\mathbf{F}_{RF} = \left[\mathbf{F}_{RF} \mid [A_{t_k_h}^T \ A_{t_k_v}^T]^T\right]$
  $\mathbf{F}_{BB} = (\mathbf{F}_{RF}^* \mathbf{F}_{RF})^{-1} \mathbf{F}_{RF}^* \mathbf{F}_{opt}$
  $\mathbf{F}_{res} = \frac{\mathbf{F}_{opt} - \mathbf{F}_{RF}\mathbf{F}_{BB}}{\|\mathbf{F}_{opt} - \mathbf{F}_{RF}\mathbf{F}_{BB}\|_F}$
$\mathbf{F}_{BB} = \sqrt{N_s} \frac{\mathbf{F}_{BB}}{\|\mathbf{F}_{RF}\mathbf{F}_{BB}\|_F}$
return $\mathbf{F}_{RF}$, $\mathbf{F}_{BB}$

Algorithm 4 Hybrid beamforming using OBMP for dual-polarized antenna

Requires: $\mathbf{F}_{opt} = [\mathbf{F}_{h_opt}^T \ \mathbf{F}_{v_opt}^T]^T$ obtained by SVD, candidate matrix A_{DFT}

$\mathbf{\Psi}_h = \mathbf{A}_{DFT}^* \mathbf{F}_{h_opt}$
$\mathbf{V}_h$ = diag($\mathbf{\Psi}_h \mathbf{\Psi}_h^*$)
$index_h = argsort(\mathbf{V}_h)[0 : N_{RF}]$
$\mathbf{F}_{RF_h} = A_{DFT}[:, index_h]$
$\mathbf{\Psi}_v = \mathbf{A}_{DFT}^* \mathbf{F}_{v_opt}$
$\mathbf{V}_v$ = diag($\mathbf{\Psi}_v \mathbf{\Psi}_v^*$)
$index_v = argsort(\mathbf{V}_v)[0 : N_{RF}]$
$\mathbf{F}_{RF_v} = A_{DFT}[:, index_v]$
$\mathbf{F}_{RF} = [\mathbf{F}_{RF_h} \mid \mathbf{F}_{RF_v}]$
$\mathbf{F}_{BB} = (\mathbf{F}_{RF}^* \mathbf{F}_{RF})^{-1} \mathbf{F}_{RF}^* \mathbf{F}_{opt}$
$\mathbf{F}_{BB} = \sqrt{N_s} \frac{\mathbf{F}_{BB}}{\|\mathbf{F}_{RF}\mathbf{F}_{BB}\|_F}$
return $\mathbf{F}_{RF}$, $\mathbf{F}_{BB}$

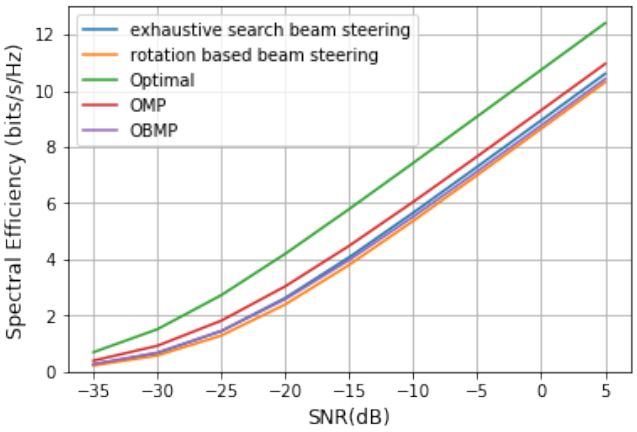

Fig. 5: Spectral efficiency of different techniques in the channel with $N_c = 6$, $N_{ray} = 2$

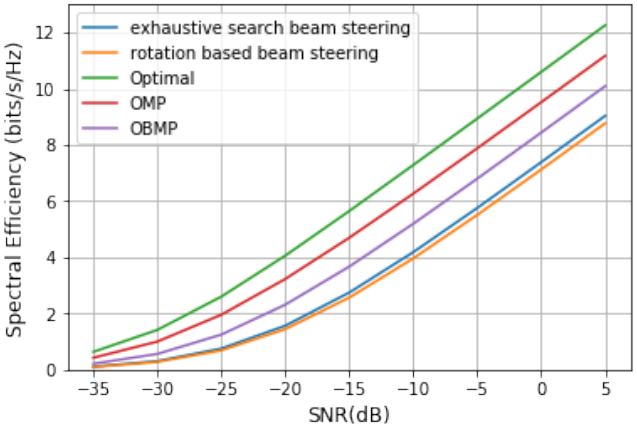

Fig. 6: Spectral efficiency of different techniques in the channel with $N_c = 6$, $N_{ray} = 10$

following by OBMP and they exceed the data rate of beam steering technique.

For the computational complexity analysis of these 4 proposed techniques, rotation based beam steering is the least complex. It looks for the best combination in the set of $N_c \times N_{ray}$ candidates in the same ray category or $N_c \times N_{ray} \times (N_c \times N_{ray} - 1)$ candidates in the different ray category. For exhaustive search beam steering, the number of candidates are from all 3 categories and equals to $N_c \times N_{ray} \times (2N_c \times N_{ray} - 1)$. Then it is slightly more than double the computations of rotation based beam steering. The 2 other algorithms OMP and OBMP have more computational complexity noting that the matrix conversion of an $N \times N$ matrix has a complexity of $O(N^3)$. If we consider this step as the most important for the complexity, OBMP can reduce the computations of OMP technique by N_{RF} times.

VI. Conclusion

In this paper, two popular hybrid beamforming techniques for omnidirectional antenna are introduced for dual-polarized antenna - the beam steering technique and the OMP technique. Their developed version to reduce the computational complexity are also proposed. For beam steering technique, we proposed searching for the best combination of paths in just one category rather than in all threes, based on the mobile rotation. Based on OMP, the OBMP technique is introduced to avoid the iteration process and the pseudo inverse. This technique does not need the AoDs information which is hard to obtain in reality. Two simulations are done in two scenario: high number and small number of path rays in the channel. We conclude that in the channel with small number of rays, these four proposed methods are close to each others. In channel with high number of rays, the two methods based on OMP exceeds the performance of two methods based on beam steering.

References

[1] T. S. Rappaport, S. Sun, R. Mayzus, H. Zhao, Y. Azar, K. Wang, G. N. Wong, J. K. Schulz, M. Samimi, and F. Gutierrez, "Millimeter wave mobile communications for 5g cellular: It will work!," *IEEE Access*, vol. 1, pp. 335–349, 2013.

[2] S. K. Yong and C.-C. Chong, "An overview of multigigabit wireless through millimeter wave technology: Potentials and technical challenges," *EURASIP Journal on Wireless Communications and Networking*, vol. 2007, p. 078907, Dec 2006.

[3] A. F. Molisch, V. V. Ratnam, S. Han, Z. Li, S. L. H. Nguyen, L. Li, and K. Haneda, "Hybrid beamforming for massive mimo: A survey," *IEEE Communications Magazine*, vol. 55, no. 9, pp. 134–141, 2017.

[4] R. Méndez-Rial, C. Rusu, N. González-Prelcic, A. Alkhateeb, and R. W. Heath, "Hybrid mimo architectures for millimeter wave communications: Phase shifters or switches?," *IEEE Access*, vol. 4, pp. 247–267, 2016.

[5] O. E. Ayach, R. W. Heath, S. Abu-Surra, S. Rajagopal, and Z. Pi, "The capacity optimality of beam steering in large millimeter wave mimo systems," in *2012 IEEE 13th International Workshop on Signal Processing Advances in Wireless Communications (SPAWC)*, pp. 100–104, June 2012.

[6] O. E. Ayach, S. Rajagopal, S. Abu-Surra, Z. Pi, and R. W. Heath, "Spatially sparse precoding in millimeter wave mimo systems," *IEEE Transactions on Wireless Communications*, vol. 13, pp. 1499–1513, March 2014.

[7] A. A. Khalek, R. W. Heath, S. Rajagopal, S. Abu-Surra, and J. C. Zhang, "Cross-polarization rf precoding to mitigate mobile misorientation and polarization leakage," in *2014 IEEE 11th Consumer Communications and Networking Conference (CCNC)*, pp. 581–586, Jan 2014.

[8] O. E. Ayach, S. Rajagopal, S. Abu-Surra, Z. Pi, and R. W. H. Jr., "Spatially sparse precoding in millimeter wave MIMO systems," *CoRR*, vol. abs/1305.2460, 2013.

[9] J. A. Tropp and A. C. Gilbert, "Signal recovery from random measurements via orthogonal matching pursuit," *IEEE Transactions on Information Theory*, vol. 53, pp. 4655–4666, Dec 2007.

[10] S. J. Wright, R. D. Nowak, and M. A. T. Figueiredo, "Sparse reconstruction by separable approximation," *IEEE Transactions on Signal Processing*, vol. 57, pp. 2479–2493, July 2009.

[11] W. Hung, C. Chen, C. Liao, C. Tsai, and A. A. Wu, "Low-complexity hybrid precoding algorithm based on orthogonal beamforming codebook," in *2015 IEEE Workshop on Signal Processing Systems (SiPS)*, pp. 1–5, Oct 2015.

[12] G. Kizer, *Digital Microwave Communication: Engineering Point-to-Point Microwave Systems*. John Wiley & Sons, 2013.